photonics

Article

Harnessing Multistability: A Novel Approach to Optical Logic Gate Construction Using Erbium-Doped Fiber Lasers

Safara Bibi [1], Guillermo Huerta-Cuellar [1,*,†], José Luís Echenausía-Monroy [2,†], Rider Jaimes-Reátegui [1,†], Juan Hugo García-López [1] and Alexander N. Pisarchik [3,*]

1 Dynamical Systems Laboratory, CULagos, Universidad de Guadalajara, Centro Universitario de los Lagos, Enrique Díaz de León 1144, Paseos de la Montaña, Lagos de Moreno 47460, Mexico; safara.bi9231@alumnos.udg.mx (S.B.); rider.jaimes@academicos.udg.mx (R.J.-R.); jhugo.garcia@academicos.udg.mx (J.H.G.-L.)
2 Applied Physics Division, Center for Scientific Research and Higher Education at Ensenada, CICESE, Carr. Ensenada-Tijuana 3918, Zona Playitas, Ensenada 22860, Mexico; echenausia@cicese.mx
3 Center for Biomedical Technology, Universidad Politécnica de Madrid, Campus Montegancedo, 28223 Madrid, Spain
* Correspondence: guillermo.huerta@academicos.udg.mx (G.H.-C.); alexander.pisarchik@ctb.upm.es (A.N.P.)
† These authors contributed equally to this work.

Abstract: We present an innovative method harnessing multistability within a diode-pumped erbium-doped fiber laser to construct logic gates. Our approach involves manipulating the intensity of external noise to regulate the probability of transitioning among four concurrent attractors. In this manner, we facilitate the realization of OR, AND, NOR, and NAND logic operations, aligning with the coexisting period-1, period-3, period-4, and period-5 orbits. Employing detrended fluctuation analysis, we establish equilibrium in the probability distributions of these states. The obtained results denote a substantial advancement in the field of optical logic gate development, representing a pivotal stride toward the seamless integration of an all-optical logic gate within laser oscillator-based systems.

Keywords: multistate intermittency; multistability; erbium-doped fiber laser; detrended fluctuation analysis; logic operations; logic gates

Citation: Bibi, S.; Huerta-Cuellar, G.; Echenausía-Monroy, J.L.; Jaimes-Reátegui, R.; García-López, J.H.; Pisarchik, A.N. Harnessing Multistability: A Novel Approach to Optical Logic Gate Construction Using Erbium-Doped Fiber Lasers. *Photonics* **2024**, *11*, 176. https://doi.org/10.3390/photonics11020176

Received: 20 December 2023
Revised: 8 February 2024
Accepted: 13 February 2024
Published: 15 February 2024

1. Introduction

Systems exhibiting multiple coexisting attractors have been identified across various scientific disciplines and in natural phenomena [1,2]. Among many dynamical systems displaying coexisting attractors, the laser marked a pivotal milestone as the first system where multistability was experimentally observed [3]. Special attention is directed towards fiber lasers due to their pivotal roles in optical communications, reflectometry, sensing, and medicine [4,5]. In particular, erbium-doped fiber lasers (EDFLs) stand out as an optical device that has captured the significant interest of numerous researchers due to their versatility. These lasers are distinguished by their compact dimensions, high damage threshold, excellent heat dissipation, and superior efficiency. Beyond their practical applications, EDFLs hold significance in the realm of nonlinear systems. Their dynamics exhibit susceptibility to external perturbations, leading to the emergence of chaos and the coexistence of multiple attractors [2,6,7].

Multistability is an intriguing phenomenon not only from a scientific standpoint but also due to its important applications, including advancements in cognitive neuroscience [8–10], generation of giant pulses [11], secure communications [12,13], and digital computing [14–16]. Highlighting the last-mentioned advancements, it is noteworthy that experimental implementations of logic gates, rooted in a triple-well potential, have been successfully implemented in electronic systems [14] and cavity magnonic systems [15]. The intrinsic versatility of a triple-well potential system is demonstrated further, as it enables the attainment of all six logic operations through the combination of various states [16].

Considering the aforementioned advantages of EDFLs, coupled with their comparatively low implementation cost and straightforward experimental realization for future endeavors, the EDFL emerges as an exceptionally advantageous system for proposing and implementing optical logic gates [17,18]. In contrast to earlier logic gate implementations that relied on perturbing the laser with a digital signal, our current research delves into the influence of external noise. This enhancement streamlines the process, paving the way for the realization of four distinct logic operations. The convergence of diverse scientific domains, encompassing both attractor dynamics and logic operations, underscores the broad-reaching implications and interdisciplinary significance of these multifaceted systems.

The formulation of digital functions for characterizing logic gates within dynamical systems typically involves the integration of hybrid systems, where signals generated in a computer are translated into analog signals. The concept of "chaos computing" has gained considerable traction, leveraging the dynamic properties of chaotic systems. This approach predominantly relies on employing an analog chaotic oscillator that emulates the behavior of multiple logic gates. This unique feature enables seamless transitions between different modes of operation, facilitating the resolution of specific arithmetic operations [7]. The seminal work of Sinha et al. [19], introducing an SR (set–reset) flip-flop based on NOR gates implemented by a Chua circuit, marked the inception of extensive research and development in chaotic logic gates [18,20–23]. Noteworthy among these efforts are shared challenges, namely, (i) the utilization of systems with coexisting attractors, and (ii) the incorporation of the sum of two digital decorrelated and periodless signals as input to the dynamical system for generating the truth table associated with the logic gate. These commonalities form the foundational basis for exploring the potential and limitations of chaos-driven computing in logic gate applications.

In this study, we introduce a novel approach to implementing logic gates using noise-induced multistate intermittency (or attractor hopping) in a laser system. Our work represents the first exploration of logic gate functionality controlled by external noise in such a system. Specifically, through comprehensive numerical simulations, we demonstrate the feasibility of realizing logic gates in a noisy EDFL coupled with a low-pass filter (LPF). In our system, each logic operation is uniquely associated with a specific periodic orbit. Notably, in the laser system featuring four coexisting periodic orbits, we assign the period 1 (P1) to OR operation, period 3 (P3) to AND, period 4 (P4) to NOR, and period 5 (P5) to NAND. The conceptual representation of the potential well for such a system is illustrated in Figure 1.

The introduction of noise in this system destabilizes coexisting attractors, making the system metastable and inducing transitions between them. This offers a dynamic and adaptable foundation for logic gate operations. In the presence of noise, a laser system featuring coexisting attractors undergoes multistate intermittency, wherein the laser switches between various coexisting states [24,25].

The subsequent sections of this paper are structured as follows. Section 2 provides an overview of the laser system employed, outlining its diverse behaviors and elucidating the method employed to induce attractor hopping within the system. In Section 3, we present the results achieved by equalizing the probability of occurrence for each coexisting period in the laser. This section also delves into the process of constructing a digital signal by activating logic operations when the EDFL exhibits equiprobable multistate intermittency. In Section 4, we explore a potential experimental implementation of the proposed method and elucidate it through a schematic representation of the corresponding laser device. The final section, Section 5, encapsulates the conclusions drawn from this work and offers a platform for discussions on its implications and potential future directions.

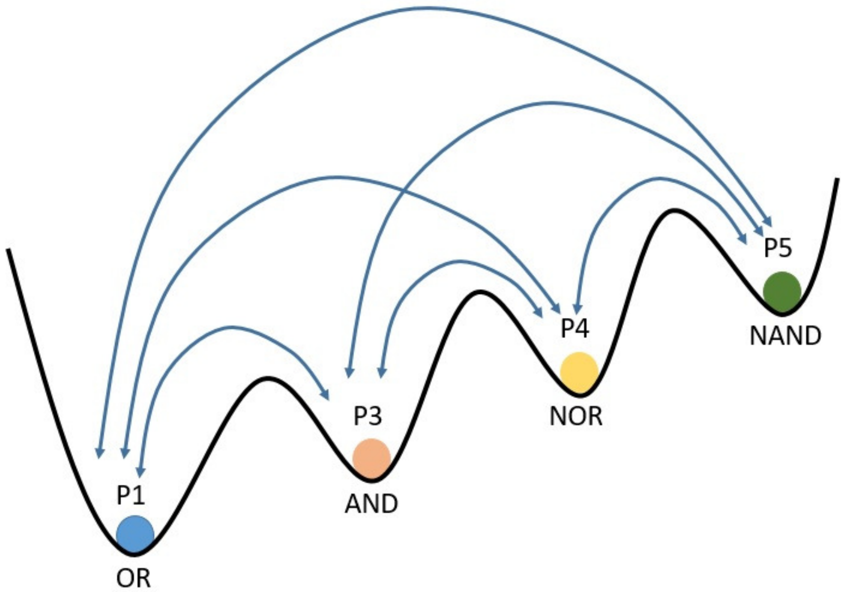

Figure 1. Hypothetical potential well for an EDFL system featuring four coexisting attractors (P1, P3, P4, P5), with noise-induced transitions between them indicated by the arrows.

2. Numerical Model of Erbium-Doped Fiber Laser

The dynamics of an EDFL is described by two differential equations [26]

$$\begin{aligned} \frac{dP}{dt} &= \frac{2L}{T_r} P\{r_w \alpha_0 [N(\zeta_1 - \zeta_2) - 1] - \alpha_{th}\} + P_{sp}, \\ \frac{dN}{dt} &= \frac{\sigma_1 r_w P}{\pi r_0^2}(N\zeta_1 - 1) - \frac{N}{\tau} + P_{pump}, \end{aligned} \tag{1}$$

where P is the power of the laser in the cavity, $N = \frac{1}{n_0 L}\int_0^L N^2(z)\,dz$ is the mean value of the upper level of the laser potential, where n_0 is the refractive index of the cold core of the erbium-doped fiber, ζ_1 and ζ_2 indicate the relationship between the effective cross sections and the fundamental absorption state, and N_2 is the upper level in the z coordinate (propagation direction of the laser emission). The element T_r is the total time required for a photon to travel through the cavity, α_0 is the absorption coefficient of the erbium-doped fiber, α_{th} is the threshold loss counter of the laser cavity, τ is the lifetime of an excited erbium ion, and r_w is the quantity that determines how closely the fundamental mode of the laser and the volume of the erbium-doped core coincide. The spontaneous emission in the laser basic regime is described by

$$P_{sp} = N\frac{10^{-3}}{T_r \tau}\left(\frac{\lambda_g}{\omega_0}\right)^2 \frac{r_0^2 \alpha_0 L}{4\pi^2 \sigma_1 2}, \tag{2}$$

where λ_g is the wavelength of the laser emission at 1.5 μm. The pump power

$$P_{pump} = P_p \frac{1 - \exp[-\alpha_0 \beta L(1-N)]}{N_0 \pi r_0^2 L} \tag{3}$$

is periodically modulated as follows:

$$P_p = p[1 - m\sin(2\pi f_m t)], \tag{4}$$

where m and f_m are the modulation depth and frequency, respectively, P_p is the dimensionless pumping power at the fiber inlet, and p is the constant power without modulation.

The system in Equation (1) is normalized to obtain the following dimensionless form [26]:

$$\begin{aligned} \dot{x} &= axy - bx + c(y + r_w), \\ \dot{y} &= dxy - (y + r_w) + e\left\{1 - \exp\left[-\beta\alpha_0 L\left(1 - y + \frac{r_w}{\zeta_2 r_w}\right)\right]\right\}, \end{aligned} \tag{5}$$

where a, b, c, and d are coefficients given in Table 1.

Table 1. Parameter values of the normalized system in Equation (5) for numerical simulations of the EDFL.

Parameter	Value	Parameter	Value
a	6.620×10^7	b	7.415×10^6
c	0.016	d	4.076×10^3
e	506	r_w	0.307
$\zeta_2 r_w$	0.615	$-\beta\alpha_0 L$	−18

These equations can be solved numerically by modulating the pump current of the laser diode with a periodic signal and analyzing the response of the laser to changes in modulation frequency and amplitude. Figure 2 shows the bifurcation diagram of the local maxima of the laser intensity obtained by varying modulation frequency f_m for fixed modulation depth $m = 1$. The frequency was changed in steps of 1 kHz, and a random initial condition was used for each change. The region of multistability explored in this paper are marked in red. One can see that at $f_m = 80$ kHz, the laser exhibits the coexistence of four stable periodic orbits (P1, P3, P4, P5).

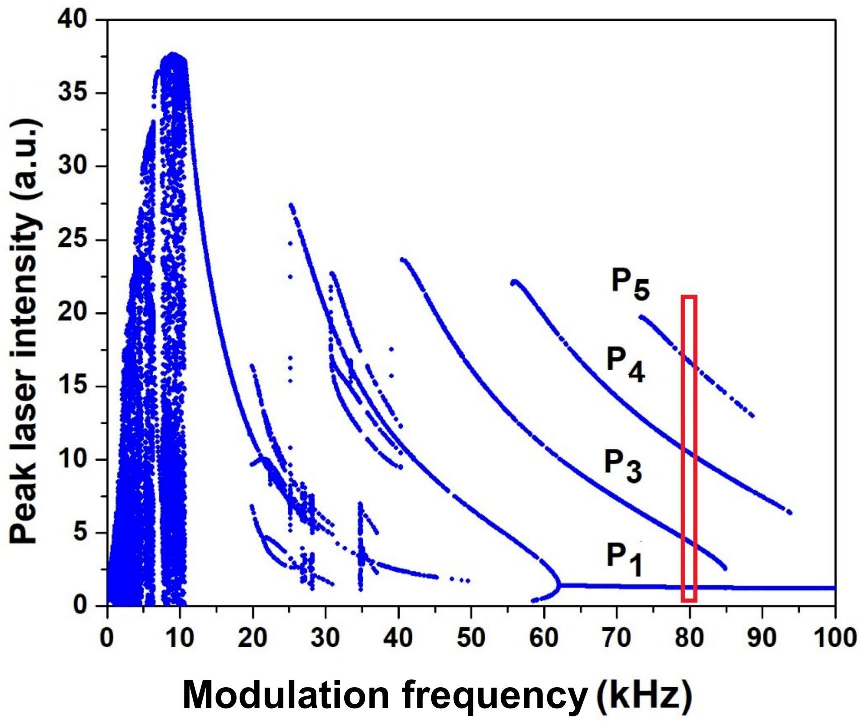

Figure 2. Numerical bifurcation diagram of Equation (5) with respect to modulation frequency f_m for $m = 1$. The red rectangle indicates the modulation frequency explored in this work.

Remark 1. *In this paper, we use the term "period" to denote the duration of a periodic orbit within the laser system. This refers to the repetitive oscillations induced by the harmonic modulation of* *the pump power. The numerical representation of the period aligns with the count of periods of the pump function in the EDFL emission.*

- *If the laser oscillates in period 1, the modulation frequency is* f_m.
- *If the laser oscillates in period 3, the modulation frequency is* $f_m/3$.
- *If the laser oscillates in period 4, the modulation frequency is* $f_m/4$.
- *If the laser oscillates in period 5, the modulation frequency is* $f_m/5$.

This relationship between the pumping frequency and the periodic response of the EDFL is illustrated with the time series in Figure 3.

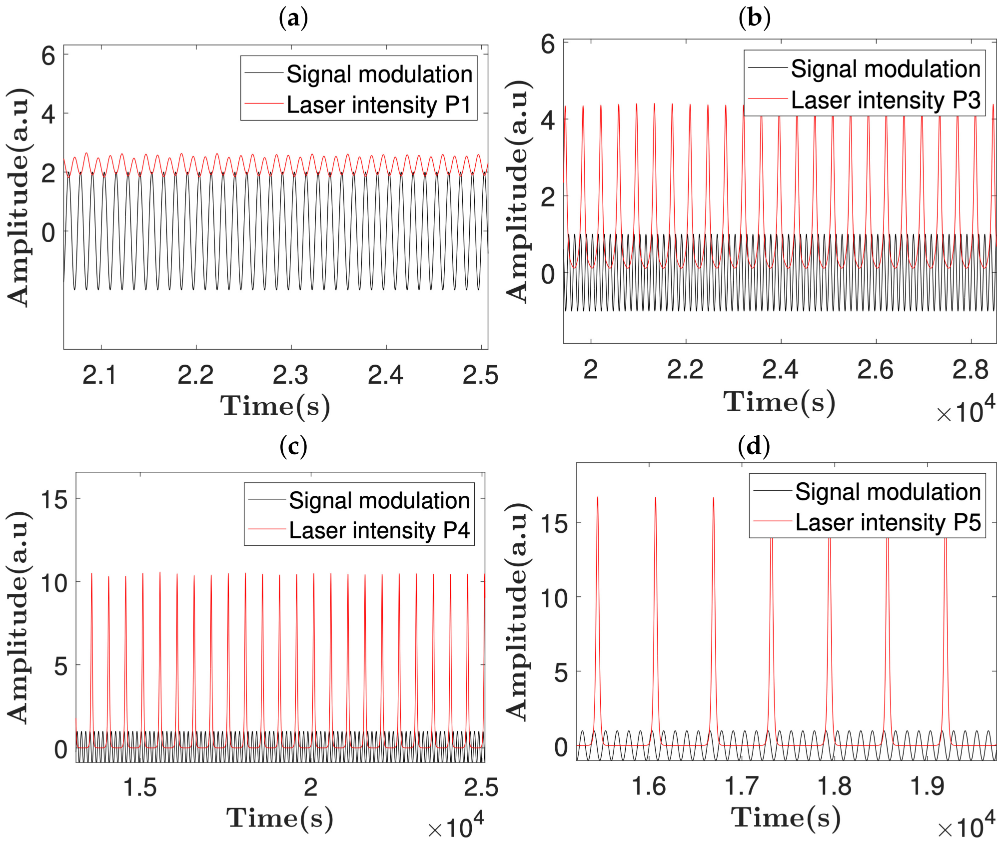

Figure 3. Time series of the laser intensity corresponding to (**a**) P1, (**b**) P3, (**c**) P4, and (**d**) P5 coexisting periodic orbits for modulation depth $m = 1$ and frequency $f_m = 80$ kHz.

2.1. System under Noise Addition

When the system described by Equation (5) is subjected to periodic modulation, the laser manifests remarkably intricate dynamics, as illustrated in Figures 2 and 3. However, adding a stochastic component to Equation (4), we obtain

$$P_p = p[1 - m\sin(2\pi f_m t) + \eta G(\xi, f_n)], \tag{6}$$

where η is the noise amplitude and $G(\eta, f_n)$ is the noise function with zero mean between a random number $\eta \in [-1, 1]$, and the frequency f_n is the low-pass filtered (LPF) noise (white noise is filtered with a discrete fifth-order low-pass Butterworth filter). In the multistability region, noise triggers multistate intermittency, also known as attractor hopping, wherein the laser alternates among the coexisting states.

The diagram in Figure 4 displays the regions of various intermittency regimes experimentally observed in the EDFL in the parameter space of the modulation frequency f_m and input noise intensity N_{in} [27]. One can note the appearance of new intermittency attractors as the input noise intensity is increased. These attractors represent the mixture of P1 and

P3 states; P1, P3, P4; and P1, P3, P4, P5; each state has different frequency, as indicated in Remark 1.

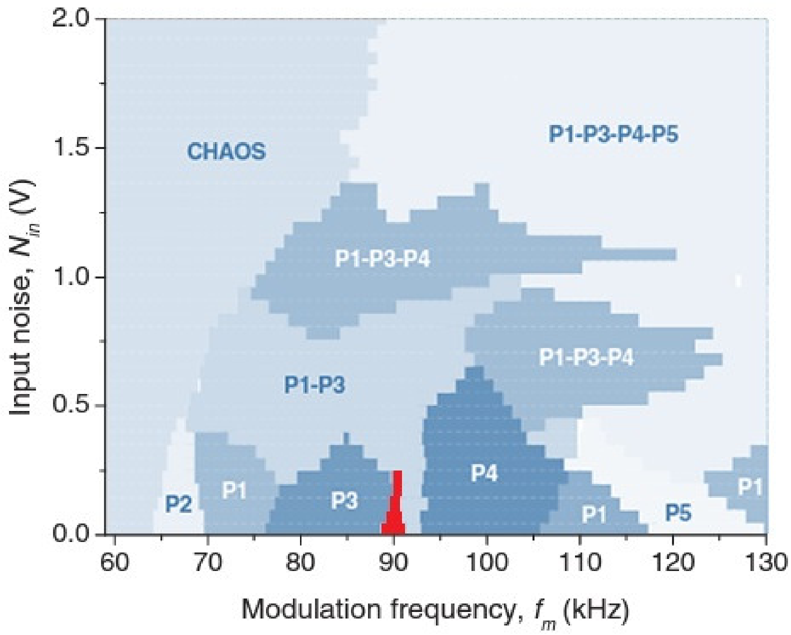

Figure 4. State diagram of the EDFL in the parameter space of modulation frequency f_m and noise intensity N_{in}. Different colors represent different periodic and metaperiodic states.

Remark 2. *While the findings presented in Figures 2 and 4 are derived from our earlier work [27], it is important to clarify that these results do not constitute the primary focus of this paper. Rather, they serve as foundational insights crucial for comprehending the contributions of the current study. As such, these results are retained within Remark 1 to provide essential context and background for the subsequent developments in this work.*

2.2. Problem Statement

As discussed in the preceding sections, the development of logic gates within dynamical systems has garnered increasing attention due to its potential advantages in information processing speed, surpassing current achievements. This approach also enables the integration of various logic gates within a single oscillator. To accomplish this, existing systems rely on decorrelated digital signals as triggers to characterize system responses and construct associated truth tables for obtained logic gates. Typically, these digital signals are generated computationally, translated into analog signals, and then injected into chaotic dynamical systems, a paradigm known as chaos computing.

In this paper, we take a distinctive approach by generating random signals derived from an optical system, such as the EDFL, operating in the regime of multistate intermittency. By stabilizing the probability of occurrence for each coexisting state within this intermittency region, the laser signal exhibits amplitude variations characteristic of each period of oscillations. This variation is leveraged to activate and randomly deactivate logic operations, facilitating the creation of digital signals implementable in optical-system-based logic gates.

3. Results

Upon the addition of a filtered noisy signal, we observe multistate intermittency previously described [2]. This phenomenon unfolds as the external noise $\eta G(\xi, f_n)$ is gradually increased. Figure 5 represent the time series of P1 (Figure 5a) and intermittent attractors (Figure 5b–d) illustrating switches between various coexisting states, derived from the LPF featuring a 60 Hz cut frequency.

While without noise ($\eta = 0$) the laser stays in one of the coexisting attractors depending on the initial conditions, say P1 (Figure 5a), increasing noise intensity induces first into two-state intermittency (switches between P1 and P3), then tri-state intermittency (switches between P1, P3, and P4), and finally multistate intermittency (switches between P1, P3, P4, and P5 [27]. To facilitate the identification of distinct periodic states in the intermittent dynamics shown in Figure 5, Table 2 provides information about noise intensity for each intermittent state.

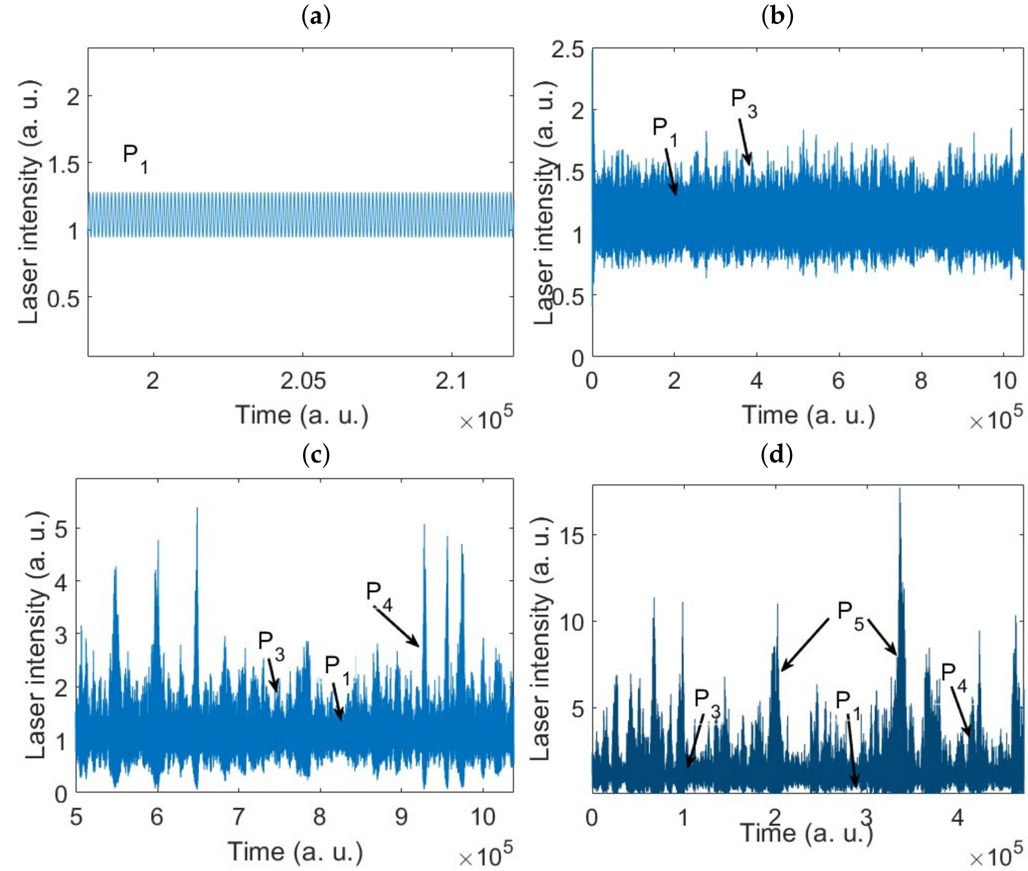

Figure 5. Time series of laser intensity after low-pass filtering at f_n = 60 kHz for noise intensities (**a**) η = 0, (**b**) η = 30, (**c**) η = 60, and (**d**) η = 80.

Table 2. Noise intensities for regimes illustrated in Figure 5.

State	Noise Intensity (a.u.)
P_1	1.5
P_3	4
P_4	8
P_5	>8

An analysis of multistate intermittency induced in the EDFL system under both periodic and stochastic modulation reveals an uneven distribution in the probability of attractor occurrences across varying noise levels. To address this discrepancy and align with the primary objective of the study—the random activation of logic operations through the laser system's hopping between coexisting states—an investigation into the system's response is undertaken for different noise intensities. This exploration aims to identify a parameter range wherein the probability of occurrence for coexisting states is comparable. By achieving a balanced distribution, any preferential bias in logic operation activation is eliminated, facilitating the generation of decorrelated digital signals by the optical system.

Remark 3. *The assignment of logic operations to each of the coexisting states of the laser is as follows:*

- *If the system has oscillations of P1 type, the OR logic operation is performed.*
- *If the system has oscillations of P3 type, the AND logic operation is performed.*
- *If the system has oscillations of P4 type, the NOR logic operation is performed.*
- *If the system has oscillations of P5 type, the NAND logic operation is performed.*

Figure 6 illustrates the assessment of each coexistent state in the EDFL for varying the noise intensity on the abscissa and LPF value on the ordinate. As outlined in Remark 3, the graphs in Figure 6 hold different logic gates. Notably, when the applied filter value f_n is below 20 kHz, the observed behavior exhibits minimal variation compared to the system without LPF, consistent with previous observations [2].

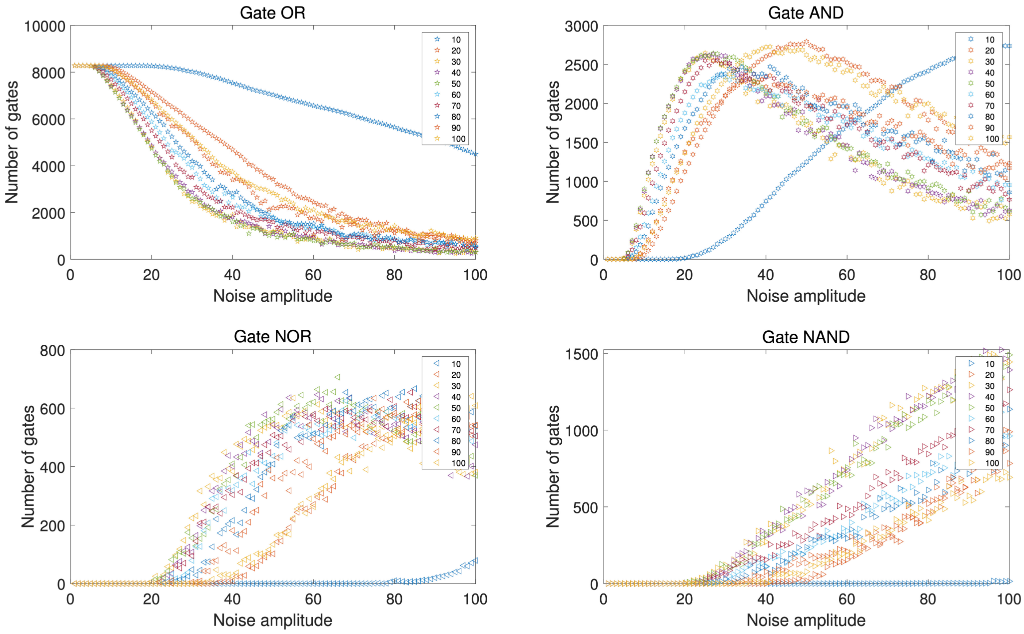

Figure 6. Number of occurrences of P1 (OR), P3 (AND), P4 (NOR), and P5 (NAND) in the multistate intermittency regime versus noise intensity for different LPF values. $f_m = 80$ kHz, $m = 1$.

Figure 7 presents the calculated probability of occurrence for each defined gate (period) based on each analyzed time series, with the color bar indicating the likelihood of a specific gate occurring in the time series for a given (η, f_n) combination.

Upon identifying the optimal range for "stabilizing" the probabilities of occurrence for different periods in the system, each period is then assigned a logic operation. This assignment triggers the activation of the corresponding operation, leading to the generation of a digital signal, intricately associated with the EDFL dynamics. The operations allocated to each period, along with their respective truth tables, are detailed in Table 3.

Table 3. Logic operations associated with each of the coexisting periods in multistate intermittency.

Inputs	OR	AND	NOR	NAND
0,0	0	0	1	1
1,0	1	0	0	1
0,1	1	0	0	1
1,1	1	1	0	0

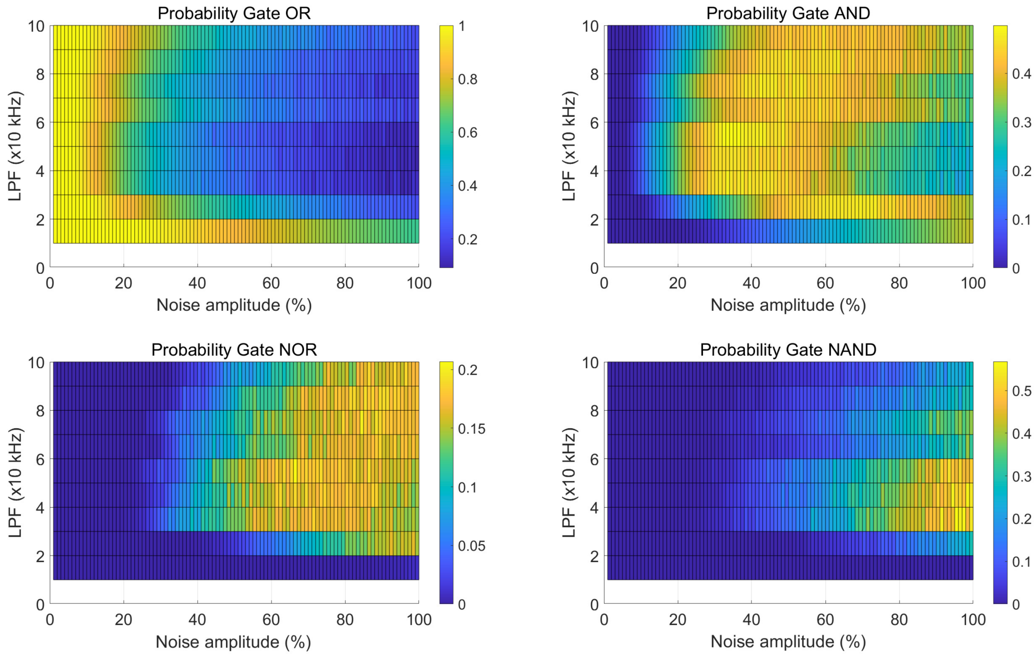

Figure 7. Probability maps of occurrence of each of the periods in the multistate intermittency regime as a function of noise intensity $\eta \times 10^{-2}$ and LPF frequency $f_n \times 10$ kHz.

The depicted behavior in Figure 7 reveals that, for specific combinations of noise intensity and particular LPF frequency, achieving a comparable probability of activating different logic gates is attainable. In light of this, we incorporate detrended fluctuation analysis (DFA). Initially introduced by Peng et al. [28], DFA elucidates long-range power-law correlations, offering insights into the statistical self-affinity of specific behaviors. This method proves valuable for analyzing time series indicative of long-memory processes, characterized by correlations in dynamical nonlinear actions (e.g., power-law decaying autocorrelation functions). Importantly, DFA helps circumvent the inadvertent detection of spurious long-range correlations stemming from nonstationarity.

The DFA analysis employs fluctuation function $F(\nu; s)$, adhering to the power-law scaling relation

$$F(\nu; s) \sim s^{\delta_\nu}, \tag{7}$$

where the time series is segmented into s pieces, each with length ν. The scaling exponent or slope δ_ν delineates distinct regimes, offering valuable insights into the laser dynamics, as follows.

- $\delta_\nu < 1/2$: anti-correlated behavior;
- $\delta_\nu \simeq 1/2$: uncorrelated behavior or white noise;
- $\delta_\nu > 1/2$: correlated behavior;
- $\delta_\nu \simeq 1$: $1/f$-noise or pink noise;
- $\delta_\nu > 1$: non-stationary or unbounded behavior;
- $\delta_\nu \simeq 3/2$: Brownian motion.

Figure 8 presents the DFA results obtained for all analyzed time series across various noise intensity variations and applied LPF frequencies. The findings affirm that the diverse combinations of amplitude noise and LPF application reflect a correlated behavior among the different interacting states within the system. Additionally, certain regions indicate proximity to pink noise behavior, suggesting nuanced dynamics in specific conditions.

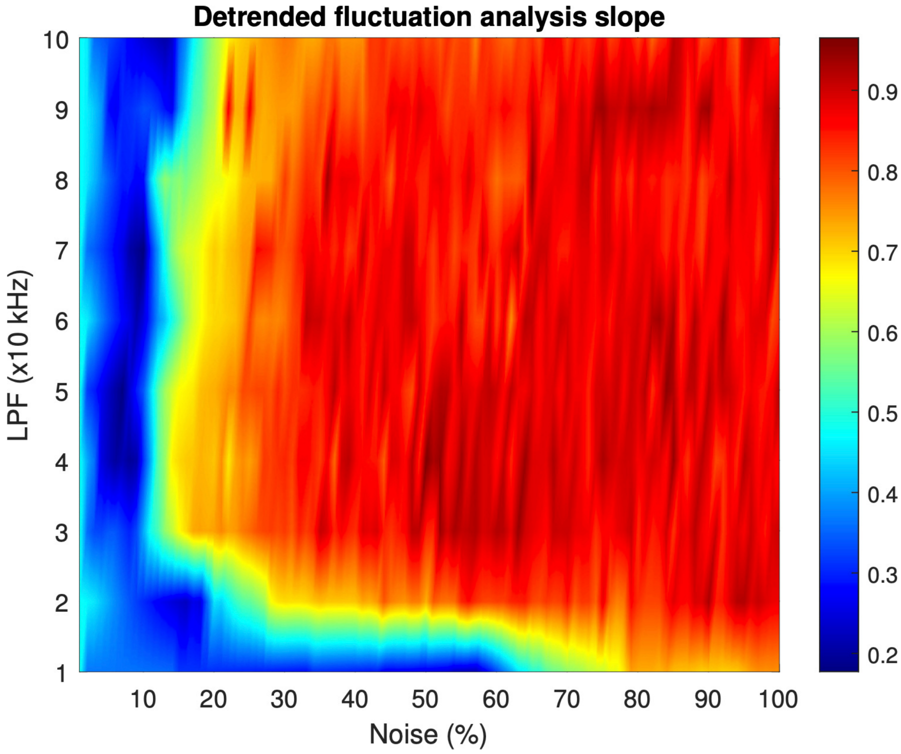

Figure 8. Map of DFA slope for each combination of noise intensity and LPF frequency. When $0.8 < \delta_v < 0.9$, a correlated behavior between P1, P3, P4, and P5 states is observed.

As an illustrative example of diverse applications, the upper trace in Figure 9a displays 300 red points that define a local maximum vector (LMV) derived from the EDFL time series with LPF at $f_n = 60$ kHz and noise intensity $\eta = 80$. The amplitude of each local maximum is employed to activate the corresponding logic gate, as outlined in Remark 4.

Remark 4. *The logic gate is determined from the waveform of the local maxima according to the following rule:*

- *If the local maxima have intensity* $I \leq 1.5$*, an OR gate is activated.*
- *If the local maxima have intensity* $1.5 < I \leq 4$*, an AND gate is activated.*
- *If the local maxima have intensity* $4 < I \leq 8$*, an NOR gate is activated.*
- *If the local maxima have intensity* $I > 8$*, an NAND gate is activated.*

Two red-square time series (Pulse I1 and Pulse I2) in the middle traces in Figure 9a depict randomly generated external digital signals, while the black-square time series (lower trace) represents the response to a logic operation (LO) between I1 and I2, defined by the LMV. To elaborate further, consider the time moment near 200 marked by a vertical blue line in Figure 9a. At this moment, the value of LMV corresponds to the AND gate, indicating the operation for $I1 = 1$ and $I2 = 0$. As expected, the result is 0, as demonstrated by the black time series of the LO in the lower trace. This example showcases the practical application of the proposed approach in executing logic operations based on the laser dynamics. Figure 9b shows a schematic representation of such a structure. It is worth mentioning that the presented result builds on earlier results of the research group that dealt with generating optical logic gates [18].

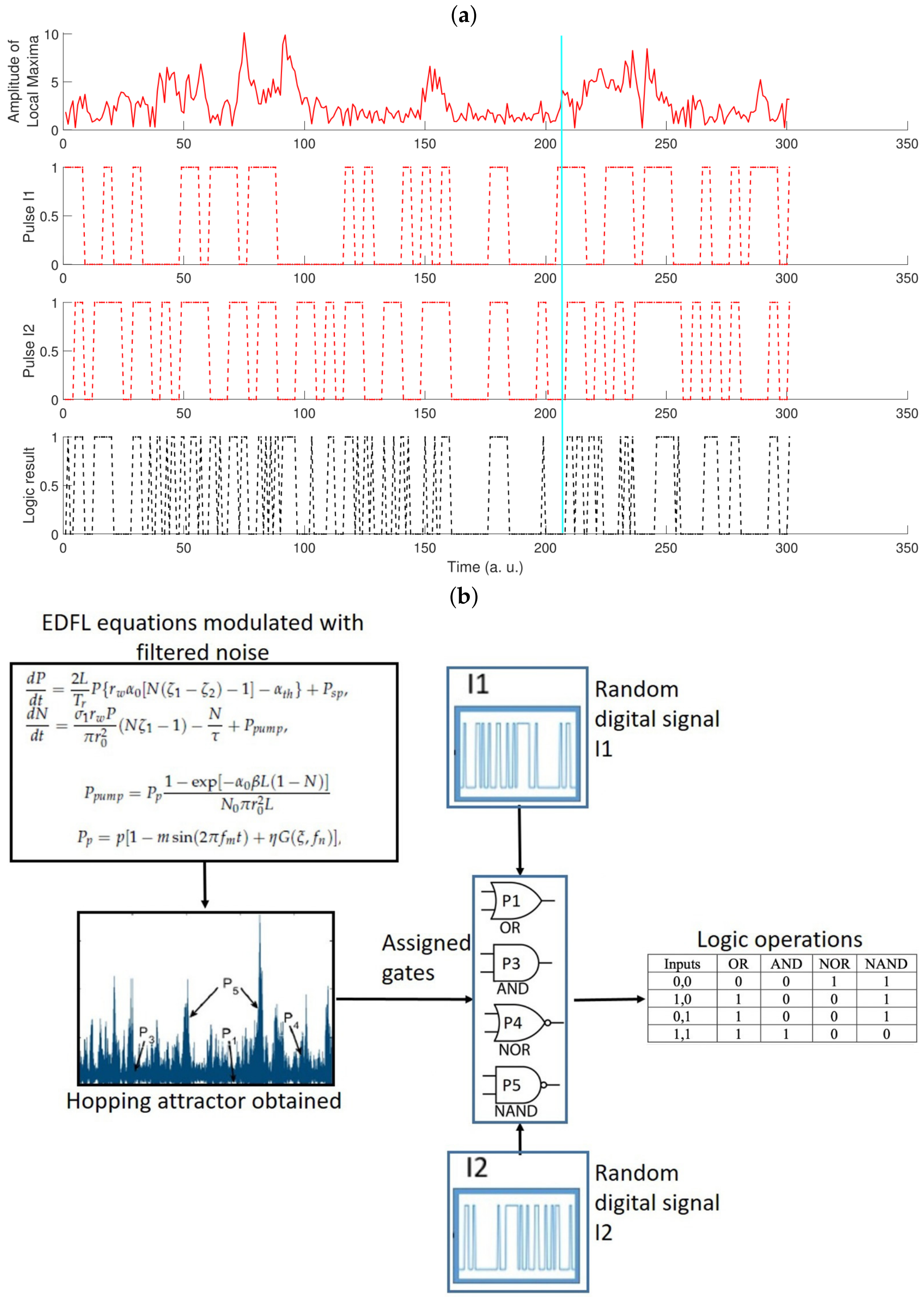

Figure 9. (**a**) Logic operations are defined by the local maxima of time series (upper trace) defining a logic gate. The squared red time series (middle traces) are two logic random signals and the black squared signal (lower trace) results from the operation defined by the laser-filtered noisy signal. (**b**) Schematic representation of the EDFL application for logic gate operations.

4. Possible Experimental Realization

The proposed method can be implemented through the experimental setup illustrated in Figure 10. A conceivable configuration incorporates key elements such as a function generator (FG) and a function noisy generator (FNG) facilitating modulation in a laser driver (LD). In the diagram, the erbium-doped fiber laser (EDFL) is delineated by black lines.

An optical isolator (OI) is employed to prevent the ingress of reflected light, preserving the laser's dynamical behavior. Subsequent to traversing the OI, the laser light impinges on a photo detector (PD), converting it into an electrical signal received by a data acquisition card (DAC).

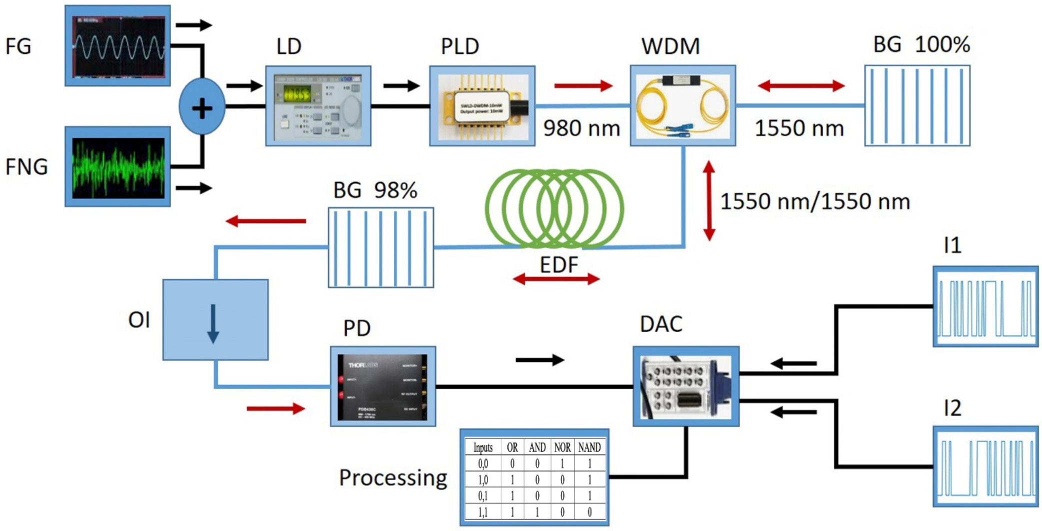

Figure 10. Schematic representation of a possible experimental implementation of logic gates using EDFL.

As previously mentioned, the EDFL exhibits very rich dynamics contingent on the modulation frequency, as illustrated with the bifurcation diagram in Figure 2. For possible experimental realization, we can set the modulation frequency at 80 kHz, where four attractors (P1, P3, P4, and P5) coexist, while the introduction of external noise will induce a multistate intermittency regime, prompting the laser to transition among these coexisting states. Reiterating an earlier point, the amplitude of each attractor in the hopping attractor determines the optical gate selection. As digital squared signals I1 and I2 enter the DAC and subsequently reach the computer (COM), digital operations specified in Table 3 can be executed.

In addition, the proposed method holds significant potential for generating pseudorandom numbers, a capability applicable across various fields such as economics, engineering, meteorology, and biology. Within cryptography, pseudorandom number generators (PRNGs) find utility in creating cryptographic keys, initialization vectors (IVs), and other essential parameters for cryptographic algorithms. In the development of video games and entertainment applications, PRNGs play a crucial role in generating random scenarios, enemies, game elements, and other dynamic aspects. Additionally, within the realm of statistics, PRNGs are instrumental in executing random sampling and simulating probability distributions. Moreover, in the domain of modeling and optimization, PRNGs serve to model and optimize intricate systems. This application extends to the design of communication networks and the optimization of routes and schedules, showcasing the versatility and broad-reaching impact of the proposed method.

5. Conclusions

In this study, we numerically explored the potential of harnessing noise-induced multistate intermittency in a multistable EDFL to realize logic gates. The manipulation of noise intensity allowed for the attainment of specific logic operations. Additionally, employing a low-pass filter for each noise variation enabled an examination of how filters can influence the probability of a particular state's occurrence. This activation of operations facilitated the generation of uncorrelated binary signals with variable periods, offering possibilities for implementation in logic gate generation schemes based on optical media.

Through the application of detrended fluctuation analysis, we revealed the correlated behavior resulting from various noise intensities combined with specific low-pass filters. This finding underscores the potential to achieve a more balanced equilibrium between different states exhibiting hopping intermittency in temporal series. Such equilibrium is valuable for applications, including encryption systems, where the generation of a pseudorandom number embedded in an optical system depends on a low-pass filter, offering enhanced security and unpredictability.

We also introduced a potential configuration for a laser device intended for the experimental implementation of optical logic gates, which we aim to carry out in the near future. An anticipated challenge in the experimental realization is the elevated level of internal noise. Nevertheless, we are optimistic about our ability to control it, drawing from our experience as demonstrated in [27].

Author Contributions: S.B.: Writing—review and editing and resources. G.H.-C.: Writing—original draft, writing—review and editing, methodology, software, validation, data curation, visualization, and project administration. J.L.E.-M.: Writing—review and editing, visualization, and conceptualization. R.J.-R.: Supervision, funding acquisition, writing—review and editing, and resources. J.H.G.-L.: Writing—review and editing, resources, and project administration. A.N.P.: Writing—review and editing and supervision. All authors have read and agreed to the published version of the manuscript.

Funding: This project was supported by CONACYT under project number 320597.

Data Availability Statement: The data related to the paper are available from the corresponding authors upon reasonable request.

Acknowledgments: J.L.E.-M. thanks CONACYT for financial support (CVU-706850, project: A1-S-26123, and project: 320597). R.J.-R. thanks CONACYT for financial support, project no. 320597.

Conflicts of Interest: The authors certify that they have NO affiliations with or involvement in any organization or entity with any financial interest (such as honoraria; educational grants; participation in speakers' bureaus; membership, employment, consultancies, stock ownership, or other equity interest; and expert testimony or patent-licensing arrangements), or nonfinancial interest (such as personal or professional relationships, affiliations, knowledge, or beliefs) in the subject matter or materials discussed in this manuscript.

References

1. Battelino, P.M.; Grebogi, C.; Ott, E.; Yorke, J.A.; Yorke, E.D. Multiple coexisting attractors, basins boundaries and basic sets. *Phys. D* **1995**, *32*, 296–305. [CrossRef]
2. Pisarchik, A.N.; Hramov, A.E. *Multistability in Physical and Living Systems: Characterization and Applications*; Springer: Cham, Switzerlands, 2022.
3. Arecchi, F.T.; Meucci, R.; Puccioni, G.; Tredicce, J. Experimental evidence of subharmonic bifurcations, multistability, and turbulence in a Q-switched gas laser. *Phys. Rev. Lett.* **1982**, *49*, 1217–1220. [CrossRef]
4. Digonnet, M. (Ed.) *Rare Earth Doped Fiber Lasers and Amplifiers*; Marcel Dekker: New York, NY, USA, 1993.
5. Okhotnikov, O.G. (Ed.) *Fiber Lasers*; Willey-VCN Verlag GmbH & Co. KGaA: Weiheim, Germany, 2012.
6. Sanchez, F.; LeFlohic, M.; Stephan, G.M.; LeBoude, P.; Francois, P.L. Quasi-periodic route to chaos in erbium-doped fiber laser. *IEEE J. Quantum Electron.* **1995**, *31*, 481–488. [CrossRef]
7. Meucci, R.; Marc Ginoux, J.; Mehrabbeik, M.; Jafari, S.; Clinton Sprott, J. Generalized multistability and its control in a laser. *Chaos* **2022**, *32*, 083111. [CrossRef] [PubMed]
8. Malashchenko, T.; Shilnikov, A.; Cymbalyuk, G. Six types of multistability in a neuronal model based on slow calcium current. *PLoS ONE* **2011**, *6*, e21782. [CrossRef] [PubMed]
9. Chen, Y.A.; Huang, T.R. Multistability of the brain network for self-other processing. *Sci. Rep.* **2017**, *7*, 43313. [CrossRef]
10. Maksimenko, V.A.; Kuc, A.; Frolov, N.S.; Khramova, M.V.; Pisarchik, A.N.; Hramov, A.E. Dissociating cognitive processes during ambiguous information processing in perceptual-decision making. *Front. Behav. Neurosci.* **2020**, *14*, 95. [CrossRef]
11. Jaimes-Reátegui, R.; Esqueda de la Torre, J.O.; García-López, J.H.; Huerta-Cuellar, G.; Aboites, V.; Pisarchik, A.N. Generation of giant periodic pulses in the array of erbium-doped fiber lasers by controlling multistability. *Opt. Commun.* **2020**, *477*, 126355. [CrossRef]
12. Yu, F.; Zhang, Z.; Liu, L.; Shen, H.; Huang, Y.; Shi, C.; Cai, S.; Song, Y.; Du, S.; Xu, Q. Secure communication scheme based on a new 5D multistable four-wing memristive hyperchaotic system with disturbance inputs. *Complexity* **2020**, *2020*, 5859273. [CrossRef]

13. Pisarchik, A.N.; Jaimes-Reátegui, R.; Rodríguez-Flores, C.; García-López, J.H.; Huerta-Cuellar, G.; Martín-Pasquín, F.J. Secure chaotic communication based on extreme multistability. *J. Frank. Inst.* **2021**, *358*, 2561–2575. [CrossRef]
14. Ashokkumar, P.; Aravindh, M.S.; Venkatesan, A.; Lakshmanan, M. Realization of all logic gates and memory latch in the SC-CNN cell of the simple nonlinear MLC circuit. *Chaos* **2012**, *31*, 063119. [CrossRef]
15. Shen, R.C.; Wang, Y.P.; Li, J.; Zhu, S.Y.; Agarwal, G.S.; You, J.Q. Long-time memory and ternary logic gate using a multistable cavity magnonic system. *Phys. Rev. Lett.* **2021**, *127*, 183202. [CrossRef]
16. Zhang, H.; Xu, Y.; Xu, W.; Li, X. Logical stochastic resonance in triple-well potential systems driven by colored noise. *Chaos* **2012**, *22*, 043130. [CrossRef] [PubMed]
17. Wang, L.A.; Chang, S.H.; F, L.Y. Novel implementation method to realize all-optical logic gates. *Opt. Eng.* **1998**, *37*, 1011–1018.
18. Jaimes-Reátegui, R.; Afanador-Delgado, S.; Sevilla-Escoboza, R.; Huerta-Cuellar, G.; García-López, J.H.; López-Mancilla, D.; Pisarchik, A. Optoelectronic flexible logic gate based on a fiber laser. *Eur. Phys. J. Spec. Top.* **2014**, *223*, 2837–2846. [CrossRef]
19. Sinha, S.; Ditto, W.L. Dynamics based computation. *Phys. Rev. Lett.* **1998**, *81*, 2156. [CrossRef]
20. Behnia, S.; Pazhotan, Z.; Ezzati, N.; Akhshani, A. Reconfigurable chaotic logic gates based on novel chaotic circuit. *Chaos Solitons Fractals* **2014**, *69*, 74–80. [CrossRef]
21. Munakata, T.; Sinha, S.; Ditto, W.L. Chaos computing: Implementation of fundamental logical gates by chaotic elements. *IEEE Trans. Circuits Syst. I* **2002**, *49*, 1629–1633. [CrossRef]
22. Cafagna, D.; Grassi, G. Chaos-based SR flip–flop via Chua's circuit. *Intern. J. Bifurc. Chaos* **2006**, *16*, 1521–1526. [CrossRef]
23. Murali, K.; Sinha, S.; Ditto, W.L.; Bulsara, A.R. Reliable logic circuit elements that exploit nonlinearity in the presence of a noise floor. *Phys. Rev. Lett.* **2009**, *102*, 104101. [CrossRef] [PubMed]
24. Moskalenko, O.I.; Koronovskii, A.A.; Zhuravlev, M.O.; Hramov, A.E. Characteristics of noise-induced intermittency. *Chaos Solitons Fractals* **2018**, *117*, 269–275. [CrossRef]
25. Murali, K.; Sinha, S.; Kohar, V.; Kia, B.; L, D.W. Chaotic attractor hopping yields logic operations. *PLoS ONE* **2018**, *13*, e0209037. [CrossRef] [PubMed]
26. Reategui, R.; Kir'yanov, A.; Pisarchik, A.; Barmenkov, Y.O.; Il'ichev, N. Experimental study and modeling of coexisting attractors and bifurcations in an erbium-doped fiber laser with diode-pump modulation. *Laser Phys.* **2004**, *14*, 1277–1281.
27. Huerta-Cuellar, G.; Pisarchik, A.N.; Barmenkov, Y.O. Experimental characterization of hopping dynamics in a multistable fiber laser. *Phys. Rev. E* **2008**, *78*, 035202. [CrossRef]
28. Peng, C.K.; Buldyrev, S.V.; Havlin, S.; Simons, M.; Stanley, H.E.; Goldberger, A.L. Mosaic organization of DNA nucleotides. *Phys. Rev. E* **1994**, *49*, 1685–1689. [CrossRef]